Alternative Scenarios of Spiral Breakup in a Reaction-Diffusion Model with Excitable and Oscillatory Dynamics

Markus Bär and Michal Or-Guil
Max-Planck-Institut für Physik komplexer Systeme, Nöthnitzer Straße 38, D-01187 Dresden, Germany
(Received 15 May 1998)

Instabilities (breakup) of spiral waves in two dimensions and their one-dimensional analogs—wave trains triggered by a specific boundary condition—leading to spatiotemporally chaotic dynamics are investigated in a simple activator-inhibitor model. These instabilities always require an absolute instability of the emitted wave trains and coincide with the Eckhaus instability for the excitable case, while for oscillatory conditions the well-known convective variant of the Eckhaus instability is found. The different cases correspond to different spiral breakup phenomenologies. [S0031-9007(99)08410-0]

PACS numbers: 82.40.Ck, 05.45.–a, 47.54.+r, 82.40.Bj

The investigation of transitions from regular patterns to spatiotemporally chaotic dynamics in extended systems remains a challenge in nonlinear physics [1]. In this Letter, we investigate the instability of spirals leading to defect-mediated turbulence within a simple reaction-diffusion model with oscillatory and excitable dynamics. This transition is known as spiral breakup (BU) and has been found in experiments in pattern forming chemical reactions [2,3] and numerical simulations in various models [4–6]. So far, there exist various, often heuristic explanations of the BU phenomenon. Most consider that the spiral core is a localized source of periodic waves. Far away from the core, the profile of the spiral approaches a planar periodic wave train with a wave number specific to the parameters of the system (wavelength selection). In general, BU is attributed to the selection of a wave number that is too small to be sustained in the system. In excitable media, it has been argued that the spiral wavelength is already too close to the minimum wavelength $\lambda_{\min}$ allowed by the dispersion relation for wave trains in 1D [7]. The complex Ginzburg-Landau equation (CGLE) describes oscillatory media near a Hopf bifurcation. A comparison of analytical results on the stability of periodic waves in 1D and simulations in 2D suggested that spirals break up when the asymptotic wave train becomes absolutely unstable [8]. More recent numerical studies indicate that the BU often precedes the absolute instability of the corresponding 1D wave train [9].

Phenomenologically, there are two different BU scenarios: while spirals in excitable media usually break near the spiral core [5], spirals in the CGLE first become unstable far away from the core. Recently, this phenomenology has been analyzed in related 1D problems (waves emitted from a boundary due to convective or curvature related terms) and explained by the appearance of a global mode that asymptotes to the absolute instability in large systems [10]. Here, a reaction-diffusion model is studied, where BU near the core had been already found under excitable conditions [6]. For oscillatory conditions, BU far away from the spiral core will be reported. The 1D analog of a spiral is constructed by employing a Dirichlet boundary condition that emits a wave train. Therein, the selected wavelength λ_{dir} is similar to the one realized in the 2D spirals in the parameter region of interest. In the excitable case, BU of the wave train occurs in contrast very close to the boundary.

Furthermore, the minimum stable wavelength $\lambda_{\min}$ of a wave train in a system with periodic boundary conditions is computed by numerical stability analysis and compared to λ_{dir} selected by the 1D sources. Two scenarios are reported: if $\lambda_{\mathrm{dir}} = \lambda_{\min}$ at the onset of instability, the instability of periodic wave trains at $\lambda_{\min}$ is assumed to be absolute. If $\lambda_{\mathrm{dir}} < \lambda_{\min}$, the instability at $\lambda_{\min}$ is convective and λ_{dir} marks the onset of absolute instability. The two cases are shown to correspond to the different BU phenomenologies. Breaking near the source indicates absence of a convective instability in the periodic waves. The opposite is true for the case of BU far away from the source. Finally, a "curvature" perturbation is applied to the 1D sources. It has a destabilizing effect on the wave trains and accounts for most of the quantitative difference between the instability of the 1D source and BU in 2D in the oscillatory case.

Here, we study a two-component model describing the dynamics of a two-component vector of functions in space $\vec{U} = (u, v)$. The actual equations are of FitzHugh-Nagumo type and describe the interaction of a fast activator (u) and a slow inhibitor (v) variable:

$$\frac{\partial u}{\partial t} = -\frac{1}{\epsilon}\, u(u-1)\left(u - \frac{b+v}{a}\right) + \Delta u\,,$$
$$\frac{\partial v}{\partial t} = f(u) - v\,, \tag{1}$$
$$f(u) = \begin{cases} 0, & 0 \le u < 1/3 \\ 1 - 6.75u(u-1)^2, & 1/3 \le u \le 1 \\ 1, & 1 < u \end{cases}.$$

The form of $f(u)$ describes a delayed production of the inhibitor and the equations have been used to model patterns in a catalytic surface reaction [11]. The change

 0031-9007/99/82(6)/1160(4)$15.00

of $f(u)$ from the standard choice $f(u) = u$ [12] lead to the discovery of spatiotemporal chaos due to BU for $\epsilon > \epsilon_{\mathrm{BU}}$ [6,13]. The parameter choice $a < 1$ yields excitable (oscillatory) behavior for $b > 0$ ($b < 0$) and $0 < \epsilon \ll 1$. In both cases, an unstable focus exists with $(u, v) = (u_0, v_0)$ in the local dynamics of Eqs. (1). In the excitable case, two more fixed points appear: $(u, v) = (0, 0)$ is the stable rest state and $(u, v) = (b/a, 0)$ is a saddle that marks the threshold of the excitable medium. Throughout this Letter, a is fixed to 0.84 and b and ϵ are varied. For simulations in 2D, zero-flux boundary conditions have been employed and a spatial (temporal) discretization of $dx = 0.196$ ($dt = 9.5 \times 10^{-3}$) has been used in an explicit Euler-scheme, convergence has been tested by runs with $dx = 0.097$ and $dt = 2.4 \times 10^{-3}$. System sizes up to 200 by 200 have been studied.

Earlier work in the excitable regime [6] revealed a transition to spatiotemporal chaos that has been preceded by a modulational instability of spiral rotation known as meandering [12]. In contrast, simulations inside the oscillatory regime ($b < -0.01$) show a direct transition from spiral rotation to spatiotemporal chaos. In this regime, BU appears first far away from the core. An example is given in Fig. 1. The stable spiral in Fig. 1a has been created just below onset of the instability. If ϵ is increased slightly, the waves acquire a visible modulation in wavelength while moving outward from the spiral center. This leads to creation of new spiral pairs far away from the core (Fig. 1c). Finally, the inner part of the initial spiral survives surrounded by a sea of small defects with irregular dynamics. The size of this remainder shrinks with increasing ϵ up to the point where it disappears completely. The same scenario is observed in experiment in the Belousov-Zhabotinsky reaction (BZR) and in CGLE simulations [2,9].

Next, a 1D analog of a spiral is studied. Empirically, it is found in the oscillatory case ($b = -0.045$), that the concentrations (u, v) in the spiral core for ϵ coincide with the unstable fixed point (u_0, v_0) just below the critical ϵ_{BU}. Consequently, the equation for u in (1) is replaced by

$$\frac{\partial u}{\partial t} = -\frac{1}{\epsilon}\, u(u-1)\left(u - \frac{b+v}{a}\right) + \frac{\partial^2 u}{\partial r^2} + \frac{G(r)}{r}\,\frac{\partial u}{\partial r}\,, \qquad \frac{\partial v}{\partial t} = f(u) - v\,, \tag{2}$$

where Dirichlet $[u(0) = u_0, v(0) = v_0]$ and zero-flux $[\partial u(L)/\partial r = \partial v(L)/\partial r = 0]$ boundary conditions are used at respective ends of the 1D system of length L. A choice $G(r) = 1$, Eq. (2) represents the radial part of Eq. (1) and the last term on the right-hand side describes the impact of curvature. For simplicity, we first neglect curvature effects and set $G(r) = 0$. The Dirichlet boundary at $r = 0$ is a source of waves similar to the core of the spiral in 2D. Note, however, that the 1D source is not equivalent to the spiral in 2D. It rather describes the radial dynamics of a target pattern emitting circular waves. The specific choice of the Dirichlet condition nevertheless selects a wavelength almost identical to the one found for spirals in 2D for parameters just below ϵ_{BU}. Space-time plots from the integration of Eqs. (2) are presented in Fig. 2 for oscillatory and excitable conditions. In both cases, the wave train emitted from the left boundary at $r = 0$ exhibit an instability upon

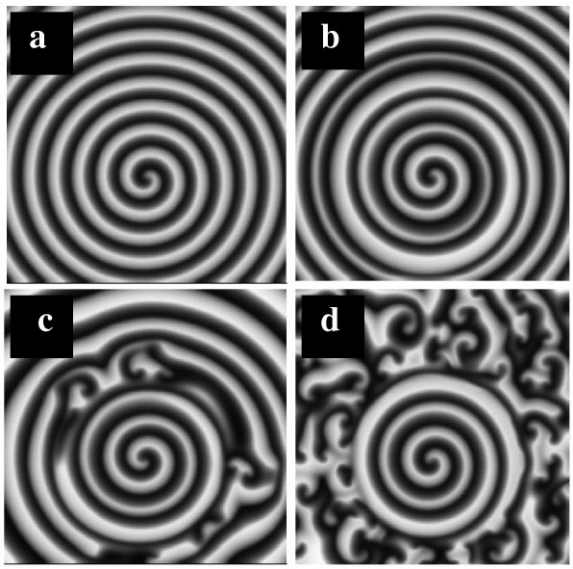

FIG. 1. BU dynamics in Eqs. (1) for ϵ slightly larger than ϵ_{BU}. Parameters are $b = -0.045$ and $\epsilon = 0.0752$. Frame (a) shows the initial spiral generated for ϵ slightly below $\epsilon_{\mathrm{BU}} = 0.075$. Frame (b) shows the modulation due to the instability, (c) is BU far away from the center and (d) is the final state, a spiral fragment surrounded by a sea of smaller defects. The frames are separated by $\delta t = 50$, system size is 100×100.

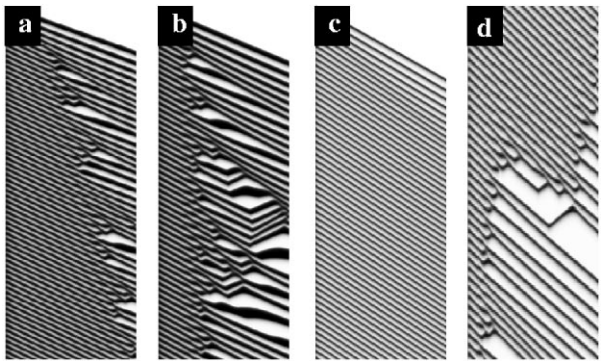

FIG. 2. Space-time plots of integrations of Eqs. (2) with $G(r) = 0$. Time is running from top to bottom, space from left to right. The length is $L = 100$, time interval shown is ≈ 250. $a = 0.84$, in all cases, $b = -0.045$ in (a), (b) and $b = 0.07$ in (c), (d). $\epsilon = 0.078$ (a), 0.082 (b), 0.081 (c), and 0.082 (d). In (a) a stable wave train is established in the long run, in (b) waves break roughly three wavelengths away from the boundary.

increase of ϵ at a critical value of ϵ_C. For $b = -0.045$, perturbations are "advected" out of the systems in line with intuitions about convective instability for ϵ just below ϵ_C (Fig. 2a). The instability manifests itself first in wave train "breakup" several wavelengths away from the boundary, as shown in Fig. 2b. In the excitable case with $b = 0.07$, the instability appears very close to the source (see Fig. 2d). The transition between the two scenarios happens around $b = 0.04$. The values of ϵ_C are not very sensitive to changes in b and lie slightly above 0.08. Thus, we find the counterpart of BU near [6] and far away from the spiral core (see Fig. 1) in the 1D model. In particular, different scenarios do not depend on 2D ingredients like meandering.

We now turn to a numerical stability analysis of wave trains. The linear stability problem for a traveling wave solution with constant shape $\vec{U}_0(r - ct)$ and constant speed c in 1D is formulated in the moving frame $z = r - ct$, in which the wave solutions are stationary. The numerical stability analysis of wave trains is performed in the 1D version of Eqs. (1) with periodic boundary conditions as the closest approximation to the unbounded system with $L = \infty$. The evolution of perturbations to $\vec{U}_0$ is described by $\vec{W}_{jn}(z)e^{\omega_{jn}t}$, where $\vec{W}_{jn}$ and ω_{jn} are eigenvectors and eigenvalues obtained from linear stability analysis. There are infinitely many eigenvalues and eigenfunctions. For $L = \infty$, ω_{jn} are located on continuous curves in the complex plane. The solution is stable when all eigenvalues ω_{jn} have negative real parts. The ring length L is used as a bifurcation parameter. The computations are done in a pseudospectral discretization of the original equations using 200 modes and 1024 collocation points. Discretization introduces a cutoff on the wave number of the eigenfunctions. In addition, the finite length L of the ring imposes a "quantization" of $2\pi/L$ on the wave numbers of the eigenfunctions. For a wave train with given wavelength λ, this finite size effect can be reduced by increasing the number N of pulses under consideration, where $L = N\lambda$. To achieve reasonable convergence of the stability properties of the wave trains, a basic solution with $N > 8$ pulses on the ring has to be used. Usage of only a single pulse results in a value of $\lambda_{\min}$ that is 10%–15% too small. Similar arguments apply to spirals in 2D, here usage of $L = 200$ corresponds to having roughly ten pulses from the core to the boundaries, and thus finite size effects on the BU instability [13] are negligible. Symmetry arguments require the eigenfunctions of the periodic operator, obtained by linearization around a solution with wavelength λ, to be Bloch functions $\vec{W}_{jn}(z) = e^{i(2\pi n/L)z}\vec{\Phi}_{jn}(z)$ with $\vec{\Phi}_{jn}(z) = \vec{\Phi}_{jn}(z + \lambda)$ with $n = 0, ..., N - 1$ [14]. Moreover, the translational symmetry of the wave trains is reflected in an eigenvector $\vec{W}_{00} = (\partial u_0/\partial z, \partial v_0/\partial z)$ with zero eigenvalue (Goldstone mode, Fig. 3). The eigenvectors corresponding to the eigenvalues with the largest real part are modulations of the Goldstone mode of the approximate form $\vec{W}_{0n} \approx e^{i(2\pi n/L)z}\vec{W}_{00}(z)$ (Fig. 3). The amplitudes of the eigenfunctions are largest in the fronts and backs of the pulses in the wave train in contrast to the Fourier eigenfunctions in the CGLE [8].

Thus, the fastest growing modes correspond to an alternating compression and expansion of subsequent pulses in line with the observations in the 2D simulations of Fig. 1b and experiments in the BZR [2]. The calculations reveal an instability reminiscent of the Eckhaus instability. As the length of the ring is shortened, the spectra of the wave trains shift towards larger real parts and cross the imaginary axis at $L_{\min} = N\lambda_{\min}(N)$ (Fig. 4). The spectra for the case $b = 0.07$ look similar to the ones in Fig. 4, but develop four maxima instead of two just below $L_{\min}$. For given parameters a and b, we have computed the $\lambda_{\min}(\epsilon)$ and compared the values with the wavelength selected by the Dirichlet source, $\lambda_{\text{dir}}(\epsilon)$. The two curves merge for $b = 0.07$ at $\epsilon = \epsilon_C$ (lower panel in Fig. 5) and cross for $b = -0.045$ for $\epsilon < \epsilon_C$ (upper panel in Fig. 5). The curves for the spiral wavelength in 2D, λ_0 are also plotted in the upper frame of Fig. 5. The BU in 2D appears at smaller values of ϵ, though the selected wavelengths of the spirals and the Dirichlet sources are almost identical just before BU. The results of Fig. 5 can be interpreted as follows: for $b = 0.07$, the instability at $\lambda_{\min}$ is absolute for ϵ_C and for $b = -0.045$ it is only convective. The periodic boundaries detect both types of instabilities, while the Dirichlet boundary condition suppresses the convective instability as already observed in the CGLE [8,10,15].

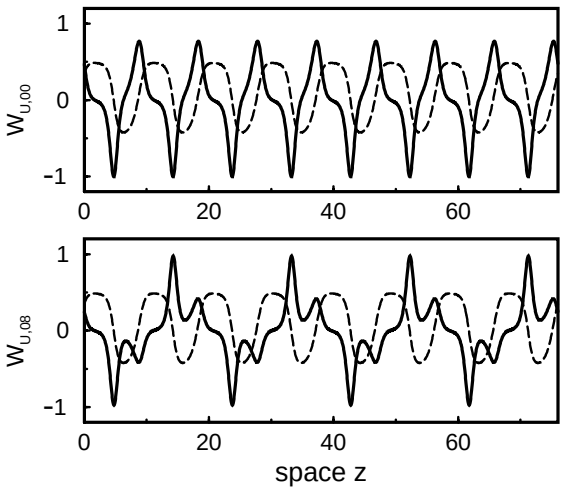

FIG. 3. Examples of eigenfunctions for $a = 0.84$, $b = -0.045$, $\epsilon = 0.081$, and $L = 152$ where $L < L_{\min} = 164.48$. Only the first half of the system length is displayed. Both eigenfunctions repeat the same pattern once more. The upper frame shows the u component of the Goldstone mode $\vec{W}_{00}$ (full line). The dashed line is the u component of the profile. The lower frame shows the real part of the u component for the eigenfunction $\vec{W}_{08}$, which corresponds to the ω_{jn} with the largest positive real part.

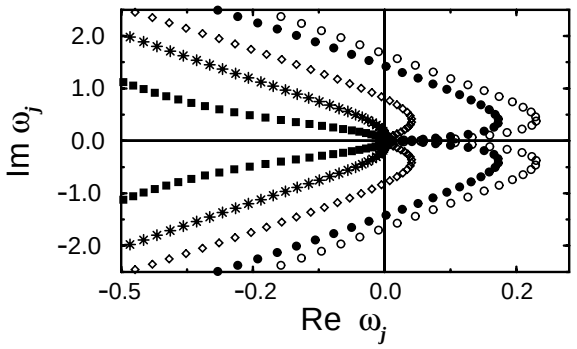

FIG. 4. Leading part of the spectra ω_{jn} for parameters of Fig. 3 and various length: $L = 114$ (open circles), $L = 122$ (full circles), $L = 142$ (diamonds), $L = 166$ (stars), and $L = 238$ (squares). $L_c \approx 164.5$ corresponding to $\lambda_{\min} \approx 10.28$.

Thus, the different scenarios depend on the presence or absence of a convective instability.

Finally, we estimate the effect of curvature by using a function $G(r) = \Theta(r - r_0)$ in Eq. (2), where Θ is the Heaviside function. The natural choice would have been $G(r) = 1$ yielding the radial part of the 2D Laplacian in Eq. (2). Usage of $G(r) = 1$, however, increases the selected wavelength substantially and prevents the instability seen in Fig. 2. Thus, we empirically determined the smallest r_0 value ($r_0 = 3.5$) that had no impact on the wavelength selection of the Dirichlet source and repeated the simulation to determine the change of ϵ_C. The critical values shift in both cases from $\epsilon_C = 0.0815$ to $\epsilon_C^{\text{curv}} = 0.076$ (see Fig. 5). This is almost identical with $\epsilon_{\text{BU}} = 0.075$ for $b = -0.045$ (Fig. 5). For $b = 0.07$, $\epsilon_{\text{BU}} = 0.0705$ is still not reached due to the impact of the meander instability on the BU [6]. Thus, the impact of curvature on the outgoing waves away from the center is crucial and accounts for most of the difference in the onset of instability in 1D and 2D for almost identical selected wave numbers.

We have investigated a reaction-diffusion model with two different BU scenarios. Both scenarios are also found for a wave emitting source triggered by suitable boundary conditions in 1D. The oscillatory case shows the familiar BU far away from the core and is related to the convective nature of the Eckhaus instability preceding the global mode instability necessary for BU. The main new finding is that BU near the core typical for excitable media stems from a variant of the Eckhaus instability that coincides with the appearance of a global mode and is related to the continuous spectrum of the spirals. Our methodology does not depend on knowledge of analytical solutions to the PDE and should be applied to other reaction-diffusion systems of interest.

We thank M. Falcke, Y. Kevrekidis, and S. Tobias for stimulating discussions and A. Bangia for programming the numerical stability code.

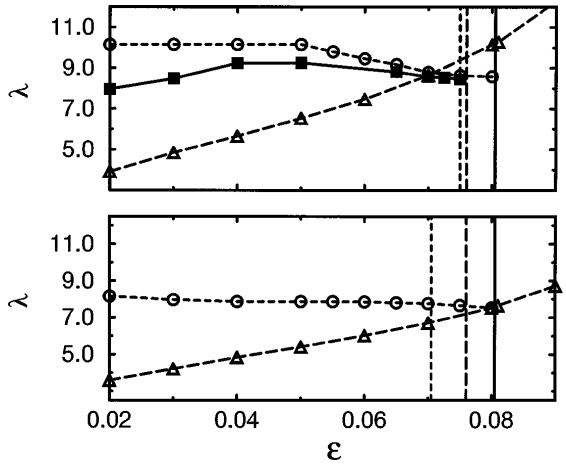

FIG. 5. Comparison of λ_{dir} (circles), $\lambda_{\min}$ (triangles), and spiral wavelength λ_0 (squares upper panel) as a function of ϵ for $b = -0.045$ (upper panel) and $b = 0.07$ (lower panel). The vertical lines indicate the values of ϵ_C (solid), ϵ_C^{curv} (long dashed), and ϵ_{BU} (dashed).

[1] M. C. Cross and P. C. Hohenberg, Rev. Mod. Phys. **65**, 851 (1993); Science **263**, 1569 (1994).
[2] Q. Ouyang and J. M. Flesselles, Nature (London) **379**, 143 (1996).
[3] S. Jakubith, H. H. Rotermund, W. Engel, A. von Oertzen, and G. Ertl, Phys. Rev. Lett. **65**, 3013 (1990); G. Veser, F. Esch, and R. Imbihl, Catal. Lett. **13**, 371 (1992).
[4] Y. Kuramoto, *Chemical Oscillations, Waves and Turbulence* (Springer, Berlin, 1984); P. Coullet, L. Gil, and J. Lega, Phys. Rev. Lett. **62**, 1619 (1989).
[5] M. Courtemanche and A. T. Winfree, Int. J. Bifurcation Chaos Appl. Sci. Eng. **1**, 431 (1991); A. Panfilov and P. Hogeweg, Phys. Lett. A **176**, 295 (1993); A. Karma, Chaos **4**, 461 (1994).
[6] M. Bär and M. Eiswirth, Phys. Rev. E **48**, 1635 (1993).
[7] E. Meron, Phys. Rep. **218**, 1 (1992).
[8] I. Aranson, L. Aranson, L. Kramer, and A. Weber, Phys. Rev. A **46**, 2992 (1992).
[9] H. Chate and P. Manneville, Physica (Amsterdam) **224A**, 348 (1996).
[10] S. M. Tobias and E. Knobloch, Phys. Rev. Lett. **80**, 4811 (1998); S. M. Tobias, M. R. E. Proctor, and E. Knobloch, Physica (Amsterdam) **113D**, 43 (1998).
[11] M. Bär, N. Gottschalk, M. Eiswirth, and G. Ertl, J. Chem. Phys. **100**, 1202 (1994).
[12] D. Barkley, Physica (Amsterdam) **49D**, 61 (1991); Phys. Rev. Lett. **68**, 2090 (1992).
[13] M. C. Strain and H. S. Greenside, Phys. Rev. Lett. **80**, 2306 (1998).
[14] N. A. Ashcroft and N. D. Mermin, *Solid State Physics* (Saunders College, Philadelphia, 1976).
[15] R. J. Deissler, J. Stat. Phys. **40**, 371 (1985).